

3D organization of chicken genome demonstrates evolutionary conservation to extreme environments

Dan Shao¹, Yu Yang¹, Shourong Shi², and Haibing Tong²

¹College of Animal Science, Shanxi Agricultural University

²Chinese Academy of Agricultural Sciences Poultry Institute

September 15, 2022

Abstract

High-through chromosome conformation capture (Hi-C) technique is widely used to study the functional roles of the three-dimensional (3D) genome architecture of genomes. However, knowledge of 3D genome structure and its dynamic during extreme environments adaption remain poor. Here we characterized 3D genome architectures with Hi-C technique for chicken liver cells. By comparing Lindian chicken (LDC) liver cells with Wenchang chicken (WCC) liver cells, we discovered that environmental adaption contributed to the switching of A/B compartments, the reorganization of topologically associated domains (TADs) and TAD boundaries in both liver cells. Besides, analysis of the switching of A/B compartments combined with liver transcriptome revealed the corresponding changes of gene expression were strongly associated with extreme environment adaption-related pathways, including Tight junction, Notch signaling pathway, Vascular smooth muscle contraction, RIG-I-like receptor signaling pathway and Glycosphingolipid biosynthesis pathways. This study advanced our understanding of evolutionary role of chicken 3D genome architecture and their significance in genome activity and transcriptional regulation.

1 Introduction

Chickens were domesticated from red jungle fowl subspecies *Gallus gallus spadiceus* ~6,000 - 8,000 years ago in South and Southeast Asia (Larson and Fuller, 2014; Miao et al., 2013; Wang et al., 2020). Subsequently, numerous indigenous local breeds were formed after a long period of natural and artificial selection, and have evolved genetic adaption to a wide range of eco-geographic conditions, especially those in tropical and frigid, and high-altitude regions (Lawal et al., 2018). As we all know, environmental pressure is an important driver shaping the animal genome, so the detection of genomic differences can clarify the genetic basis of adaptation to diverse environments and provide insights into functionally important genetic variants (Andersson and Georges, 2004; Shi et al., 2022). Meanwhile, considering their short reproductive and growth periods and wide distribution, chickens can be used as ideal models to study genetic adaptations to environments (Li et al., 2022).

To our best knowledge, genetic adaptations to naturally extreme environments in chickens have attracted many researchers, but mainly focused on high altitude adaption of Chinese chicken (Wang et al., 2015; Zhang et al., 2018b) and hot and arid environments of African and Asian chickens (Fleming et al., 2017; Tian et al., 2020) by chip analysis or whole genome analysis. There were few studies aiming at tropical and frigid environment adaption of Chinese chickens in spite of diverse Chinese local chicken breeds. In consideration of current and future global effects of climate changes (Tian et al., 2020), the genetic footprints of adaption to tropical and frigid climates in Chinese chickens are critical for modern chicken industry.

In this study, with the aim of better understanding the genetic footprints of extreme environments adaption, we applied an integrated analysis combining liver high-throughput chromosome conformation capture (Hi-C) data (Lieberman-Aiden et al., 2009) with transcriptome sequencing of Lindian chicken (LDC) and Wenchang

chicken (WCC) from two extant extreme environments (more frigid to more tropical environments). We generated genome-wide profiles of chromatin contacts using Hi-C technology, which was allowed to character spatial chromatin compartments and evaluate DNA interaction frequencies at a resolution from dozens of kilobases to megabases (Battulin et al., 2015; Veniamin et al., 2018). We identified characteristics of A/B compartments and topologically associating domains (TADs) in two different sources of livers. We also reported changes in gene expression and enriched pathways associated with the variant 3D genome, which implicated the tropical and frigid environments genetic adaptation.

2 Materials and methods

2.1 Ethical approval

The animal experiments we took all met the guidelines approved by the animal care and use committee of Poultry Institute, Chinese Academy of Agricultural Science.

2.2 Sample collection and sequencing of Hi-C experiment

According to previous studies (Barutcu et al., 2015; Battulin et al., 2015; Jiang et al., 2020), we sampled chicken livers from one Wenchang chicken (a laying hen of 43 weeks form Wenchang, Hainan), and one Lindian chicken (a laying hen of 42 weeks form Lindian, Heilongjiang) from their national natural poultry genetic resources conservation farm with tropical and frigid temperature zone, respectively. Then Chicken livers were fixed with 1% formaldehyde solution in MS buffer (10 mM potassium phosphate, pH 7.0; 50 mM NaCl; 0.1M sucrose) at room temperature for 30 min in a vacuum. After fixation, the livers were incubated at room temperature for 5 min under vacuum in MC buffer with 0.15 M glycine. Approximately 2 g fixed tissue was homogenized with liquid nitrogen and resuspended in nuclei isolation buffer and filtered with a 40-nm cell strainer to obtain liver cells. Then the procedures for enriching nuclei from flow-through and subsequent denaturation were done according to a 3C protocol established for maize.

Chromatin was digested for 16 h with 400 U HindIII restriction enzyme at 37 °C. DNA ends were labeled with biotin and incubated at 37 °C for 45 min, and the enzyme was inactivated with 20% SDS solution. DNA ligation was performed by the addition of T4 DNA ligase and incubation at 16°C for 4~6 h. After ligation, proteinase K was added to reverse cross-linking during incubation at 65 °C overnight. DNA fragments were purified and dissolved in 86µL of water. Unligated ends were then removed. Purified DNA was fragmented to a size of 300-500 bp, and DNA ends were then repaired. DNA fragments labeled by biotin were finally separated on Dynabeads® M-280 Streptavidin (Life Technologies). Hi-C libraries were controlled for quality and sequenced on an Illumina Hiseq X Ten sequencer.

2.3 Hi-C reads mapping and filtering and generation of contact matrices

Firstly, low quality paired reads (Reads with [?] 10% unidentified nucleotides (N); > 10 nt aligned to the adaptor, allowing [?] 10% mismatches; > 50% bases having phred quality < 5; and putative PCR duplicates generated in the library construction process) were removed, which mainly result from base-calling duplicates and adaptor contamination. Then the high quality paired-end Hi-C reads were mapped to Gallus_gallus-5.0 and filtered using HiCUP v0.5.10 (Steven et al., 2015). HiCUP removed sequences representing experimental Hi-C artifacts and other uninformative di-tags, since even a small number of invalid di-tags could lead to incorrect conclusions being drawn concerning genomic structure.

The genome was divided into 1Mb bins, and the read pair numbers in two regions were counted as the observed interactions by Hicpipe, and the expected interactions were also calculated by this software. The norm interactions were computed by observed interactions divided by expected interactions. We used the norm interactions for every two bins to produce norm contact matrix.

2.4 Identification of compartment A/B

Identification of compartment A/B was performed using the 1Mb interaction matrix as previously described (Wu et al., 2017). The Eigenvector value of two Hi-C samples were calculated by hiclib. Bins with positive values were defined as compartment A, otherwise B.

2.5 Generation of interchromosomal contacts matrix

The expected number of interchromosomal interactions for each chromosome pair i,j was computed by multiplying the fraction of interchromosomal reads containing i with the fraction of interchromosomal reads containing j and multiplying by the total number of interchromosomal reads. The enrichment was computed by taking the actual number of interactions observed between i and j and dividing it by the expected value.

The interchromosomal contact possibility was computed by the observed reads pairs numbers between chromosome pair i,j dividing it by its expected value. The expected number of interchromosomal interactions for each chromosome pair i,j was calculated by multiplying the proportion of interchromosomal reads containing i with the proportion of interchromosomal reads containing j and the total number of interchromosomal reads.

2.6 Identification of TADs and TAD boundaries

The normalized contact matrix was used as input to perform TAD identification as reported in mammalian (Dixon et al., 2012). Directionality index (DI) was calculated from upstream 2 Mb to downstream 2 Mb along the center of each bin at 40 kb resolution and Hidden Markov model (matlab 2013, HMM_calls.m) was then used to predict the states of DI for final TAD generation. We used the same criteria 400 kb (distance between the two adjacent TADs) to distinguish unorganized chromatin with topological boundaries, that was the topological boundaries to be less than 400 kb and unorganized chromatin to be greater than 400 kb. Transcription start sites (TSSs) were calculated based on the number of annotated genes. Firstly, the position of TAD Boundary center was obtained, and then the number of TSS in each 10 Kb window of the upstream and downstream of TAD Boundary Center with the distance delimiting size of 10 Kb was calculated.

2.7 Boundary correlation experiments

Boundary correlation was performed as previously reported (Dixon et al., 2012). We merged the center position of the boundary between two experiments of interest and calculated the directionality indexes ± 10 bins for each center. Then we randomly selected 20 bins from each of the two cell lines and calculated the spearman correlation between the two vectors. We attained the Spearman correlation coefficients distribution after repeating the randomization 10,000 times. We defined values at the top 1% of distribution as significant correlation threshold. Boundaries were identified as ‘cell type specific’ if the boundary region was in one cell and lacked a significant correlation between the LDC and WCC liver cells.

2.8 Transcriptome sequencing and analysis

Liver tissues from 8 chickens (4 LDCs of 42 weeks form Lindian, Heilongjiang and 4 WCCs of 43 weeks form Wenchang, Hainan) were collected from their national natural poultry genetic resources conservation farm and sequenced for transcriptomic analysis. Sequencing libraries were generated using NEBNext(r) UltraTM RNA Library Prep Kit for Illumina(r) (NEB, USA) following manufacturer’s recommendations and index codes were added to attribute sequences to each sample. The clustering of the index-coded samples was performed on a cBot Cluster Generation System using TruSeq PE Cluster Kit v3-cBot-HS (Illumia) according to the manufacturer’s instructions. After cluster generation, the library preparations were sequenced on an Illumina Hiseq platform and 150 bp paired-end reads were generated. Index of the reference genome (Database: Eensemble_90, version : Gallus_gallus.Gallus_gallus-5.0.dna.toplevel.fa) was built using Bowtie v2.2.3 and the high-quality RNA-seq reads were aligned to the reference genome by the HISAT2 v2.0.4 program with default parameters. HTSeq v0.6.1 was used to count the reads numbers mapped to each gene. And then Fragments Per Kilobase of transcript per Million mapped reads (FPKM) of each gene was calculated based on the length of the gene and reads count numbers (by perl script).

2.9 Enrichment analysis

For genes annotated in switched compartments A/B, we used KOBAS 2.0 software to test the statistical enrichment in KEGG pathways. Gene Ontology (GO) enrichment analysis was implemented by the Goseq

R package, in which gene length bias was corrected. GO terms with corrected P -value less than 0.05 were considered significantly.

3 Results

3.1 A comprehensive map of chromosomal contacts in chicken liver cells nuclei

To study the dynamic chromatin interactions in primary chicken liver cells from WCC and LDC, we carried out Hi-C experiments and sequenced approximately a total of 295 Gb high quality raw data. Alignment of the obtained sequences to the chicken reference genome (ftp://ftp.ensembl.org/pub/release-90/fasta/gallus_gallus/dna/) resulted in an average of ~ 263 million paired-end reads mapped for each individual, among which an average of ~ 207 million are intra-chromosomal reads (207,914,357 in LDC and 206,471,795 in WCC) (Table S1 and S2). Data processing also showed high quality of the Hi-C data, proving the successful performance of Hi-C experiments.

3.2 Identification and characterization of compartments in chicken liver cells

After data analysis, we acquired chromatin interaction heatmaps at 40-kb resolution for each sample (Fig. 1 and Fig. S1). The heatmaps displayed a typical plaid-pattern, which was demonstrated previously in chicken erythrocytes and fibroblasts Hi-C data (Veniamin et al., 2018), as well as in mammalian Hi-C data (Battulin et al., 2015). The plaid-pattern intimates the existence of large spatial compartments, such as compartments A/B. We know the genome consists of actively transcribed compartments A and inactive compartments B (Lieberman-Aiden et al., 2009), and switching of the compartments A/B are concerned with comparative changes of gene expression (Barutcu et al., 2015). We then determined the compartment types of the genome at 1 Mb resolution in liver cells, and found most genomic regions reserved the same compartments in LDC liver cells compared to WCC liver cells (Fig. 2 and Fig. 3). A total of 5% genomic regions switched between compartment A and compartment B, and as expected, we found more genes in the compartment A and they displayed higher transcriptional levels than those in compartment B (Fig. 4 and Fig. S2).

We next compared TADs in LDC and WCC liver cells. We called TADs from Hi-C interaction matrices at 40 kb resolution and identified 396, 386 TADs in LDC liver cells and WCC liver cells (Fig. 5 and Table S3), respectively, and with their median TAD sizes of 2.3 Mb (Fig. S3). Interestingly, previous studies have found TAD boundaries display an obvious enrichment of active genes when compared with randomly sampled genomic regions, which suggested a relationship between TAD formation and gene transcription (Wang et al., 2018). We thus investigated TAD boundary distribution, and 280, 261 TAD boundaries were identified in LDC and WCC genome, respectively (Table S4), with enriched transcription start sites in TAD boundary (Fig. S4), which further confirmed the reliability of the sequencing results.

3.3 Chromatin conformation and gene expression changes

We next explore the functional effects of 3D genome changes between LDC liver cells and WCC liver cells, we performed KEGG pathway analysis with genes located in the 5% genomic regions that switched between compartment B and compartment A in either direction ($A \Rightarrow B$ or $B \Rightarrow A$) in both LDC and WCC liver cells. The pathway enrichment analysis showed these genes were strongly associated with extreme environment adaption-related pathways, including Tight junction (Bethany et al., 2018; Ying et al., 2015), Notch signaling pathway (Ishida et al., 2013; Kim et al., 2019; Wang et al., 2012), Vascular smooth muscle contraction (Cardona et al., 2014), RIG-I-like receptor signaling pathway (Liu et al., 2017; Zhang et al., 2018a) (Fig. 6 and Table 1). Within the consistent A/B compartment-switching regions, we found a series of genes related to cell proliferation and differentiation in Tight junction, Notch signaling pathway and RIG-I-like receptor signaling pathway which were upregulated in A-type compartment in LDC cells comparing with WCC cells. Likewise, it should be noted that serine – threonine kinases, ie, rho-associated coiled-coil kinase isoform 2 (ROCK2), myosin light chain kinase (MYLK) in the Vascular smooth muscle contraction pathway were upregulated in A-type compartment in WCC cells.

4 Discussion

Applicating chromosome conformation capture-based high-throughput approaches has greatly promoted the presentation of spatial chromatin interaction architecture in mammals (Beagrie et al., 2017; Tjong et al., 2016). In poultry, a few studies have also attempted to discover higher-order chromatin structure using Hi-C technique (Veniamin et al., 2018). Here, we advanced a high-resolution genome-wide analysis of chromatin interactions in chicken liver cells. Our results revealed that the spatial genome organization observed in chicken cells displayed a typical paid-pattern without sharp transition between A- and B- compartments, which appeared to be similar in several previously mammalian species (Battulin et al., 2015; Dixon et al., 2012; Rao et al., 2014). In chicken, we provided the concrete evidence of genome partitioning of A/B compartments in both LDC and WCC, which was in accord with findings in chicken erythrocytes and fibroblasts (Veniamin et al., 2018).

At the TAD scale, we found that LDC hepatocyte genomes contain similar numbers of TADs and average TAD size with WCC hepatocyte. This finding was inconsistent with an earlier study between chicken erythrocytes and fibroblasts (Veniamin et al., 2018), which might attribute to their markedly different cellular properties. In support of this idea, heterogeneity of cancer cells could contribute to more diverse 3D genomes and increase the detected TAD numbers when compared with normal cells (Franke et al., 2016). We also characterized the TAD boundaries, and obtained most of the same TAD boundaries between two cells, which further confirmed accumulated tiny but not sharp genomic genetic variations that contributed to extreme environment adaption (Elbeltagy et al., 2017; Fleming et al., 2017; Zhang et al., 2018b). More studies of 3D chicken genomes will further elucidate the relationship between genome alterations and 3D genome organization.

During cell biological process, such as cell differentiation, cancer development, or stimulation response, the 3D architecture of the genome is reorganized, which is connected with changes in gene expression and epigenetic variations (Barutcu et al., 2015; Dixon et al., 2015; Rafique et al., 2015; Taberlay et al., 2016). We found that about 5% of genome regions switched between the A compartment and B compartment as making comparative analysis between LDC and WCC 3D genome, which was associated with changes in gene expression. Pathway enrichment analysis likewise illustrated that some genes located in the switched compartments were strongly associated with cell proliferation and differentiation, a common adaptive response to extreme environment (Lindsey and Tropepe, 2014; Luger et al., 2003). Not surprisingly, Tight junction and RIG-I-like receptor signaling pathway had been verified having a close relationship with heat tolerance, with an integration between metabolic and immune responses to ensure energy balance and permit growth and defense (Bethany et al., 2018; Liu et al., 2017). Interestingly, Notch signaling pathway was found not only involving in high temperature response (Liu et al., 2017), but also had a strong correlation with cold challenge (Kim et al., 2019; Wang et al., 2012), and played an extremely important role in the adaption to hypoxic environment (Ishida et al., 2013). Vascular smooth muscle contraction that includes vasoconstriction and vasodilation is a process involved in cold acclimatization (Cardona et al., 2014). Here we presented a list of cold adaption candidate genes in vascular smooth muscle contraction, among which, ROCK2 and MYLK were identified exaggerating vasoconstriction by directly phosphorylating myosin light chains (Takashima, 2009; Walsh, 1994), under these conditions, the validated interactions between ROCK2 and MYLK further demonstrated their role in environment adaption (Pasha et al., 2015). These genes in our selected pathways could be major targets for tropical and frigid environment tolerance, and many of which can be understood with further function analysis. Nonetheless, mechanisms allowing adaption to the extreme environment are expected to be complex, and our study partly provides insight into the extreme environment adaption.

5 Conclusions

In summary, this study provides the evidence that extreme environments changed the A/B compartments, reorganized the TADs and TAD boundaries of chicken 3D genome architectures. Moreover, Tight junction, Notch signaling pathway, Vascular smooth muscle contraction, RIG-I-like receptor signaling pathway and Glycosphingolipid biosynthesis pathways were suggested participating in extreme environment adaption.

Acknowledgements

This work was supported by the Jiangsu Provincial Key Laboratory of Poultry Genetics & Breeding (JQLAB-ZZ-202006).

Credit Author statements

Dan Shao : software, investigation, formal analysis, writing—Original draft /Reviewing & Editing. **Yu Yang**:conceptualization, methodology, writing—review and editing, supervision. **Shourong Shi**: conceptualization, investigation, writing—review and editing. **Haibing Tong**: validation, data curation. All authors read and approved the final version of the manuscript.

Data availability

The accession numbers for Hi-C data and transcriptome data reported in this paper are NCBI SRA (PRJNA817871) and SRA (PRJNA800119), respectively.

Competing interests

The authors declare that they have no competing interests.

Reference

- Andersson, L., and Georges, M., 2004. Domestic-animal genomics: deciphering the genetics of complex traits. *Nat. Rev. Genet.* 5, 202-212.
- Barutcu, Rasim, A., Lajoie, Bryan, R., McCord, Rachel, P., Coralee, E., Hong, Deli, and Messier., 2015. Chromatin interaction analysis reveals changes in small chromosome and telomere clustering between epithelial and breast cancer cells. *Genome Biol.* 16, 214-217.
- Battulin, N., Fishman, V. S., Mazur, A. M., Pomaznoy, M., Khabarova, A. A., Afonnikov, D. A., Prokhortchouk, E. B., and Serov, O. L., 2016. Comparison of the three-dimensional organization of sperm and fibroblast genomes using the Hi-C approach. *Genome Biol.* 17, 6-7.
- Beagrie, R. A., Scialdone, A., Schueler, M., Kraemer, D. C., Chotalia, M., Xie, S. Q., Barbieri, M., de Santiago, I., Lavitas, L. M., Branco, M. R., Fraser, J., Dostie, J., Game, L., Dillon, N., Edwards, P. A., Nicodemi, M., and Pombo, A., 2017. Complex multi-enhancer contacts captured by genome architecture mapping. *Nature* 543, 519-524.
- Bethany, D. S., Skibieli, A. L., Fabris, T. F., Zhang, Y., Dahl, G. E., Francisco, P., and Jimena, L., 2018. RNA-Seq reveals novel genes and pathways involved in bovine mammary involution during the dry period and under environmental heat stress. *Sci. Rep.* 8, 11096-11106.
- Cardona, A., Pagani, L., Antao, T., Lawson, D. J., Eichstaedt, C. A., Yngvadottir, B., Shwe, M. T., Wee, J., Romero, I. G., Raj, S., Metspalu, M., VILLEMS, R., Willerslev, E., Tyler-Smith, C., Malyarchuk, B. A., Derenko, M. V., and Kivisild, T., 2014. Genome-wide analysis of cold adaptation in indigenous Siberian populations. *PLoS One* 9, e98076.
- Dixon, J. R., Jung, I., Selvaraj, S., Shen, Y., Antosiewicz-Bourget, J. E., Lee, A. Y., Ye, Z., Kim, A., Rajagopal, N., Xie, W., Diao, Y., Liang, J., Zhao, H., Lobanenko, V. V., Ecker, J. R., Thomson, J. A., and Ren, B., 2015. Chromatin architecture reorganization during stem cell differentiation. *Nature* 518, 331-336.
- Dixon, J. R., Selvaraj, S., Yue, F., Kim, A., Li, Y., Shen, Y., Hu, M., Liu, J. S., and Ren, B., 2012. Topological domains in mammalian genomes identified by analysis of chromatin interactions. *Nature* 485, 376-380.
- Elbeltagy, A. R., Bertolini, F., Fleming, D. S., Goor, A. V., and Rothschild, M. F., 2017. Evidence of Natural Selection Footprints Among Some African Chicken Breeds and Village Ecotypes. *Front Genet.* 11.
- Fleming, D. S., Weigend, S., Simianer, H., Weigend, A., Rothschild, M., Schmidt, C., Ashwell, C., Persia, M., Reecy, J., and Lamont, S. J., 2017. Genomic Comparison of Indigenous African and Northern European

Chickens Reveals Putative Mechanisms of Stress Tolerance Related to Environmental Selection Pressure. *G3 (Bethesda)* 7, 1525-1537.

Franke, M., Ibrahim, D. M., Andrey, G., Schwarzer, W., Heinrich, V., Schopflin, R., Kraft, K., Kempfer, R., Jerkovic, I., Chan, W. L., Spielmann, M., Timmermann, B., Wittler, L., Kurth, I., Cambiaso, P., Zuffardi, O., Houge, G., Lambie, L., Brancati, F., Pombo, A., Vingron, M., Spitz, F., and Mundlos, S., 2016. Formation of new chromatin domains determines pathogenicity of genomic duplications. *Nature* 538, 265-269.

Ishida, T., Hijioka, H., Kume, K., Miyawaki, A., and Nakamura, N. (2013). Notch signaling induces EMT in OSCC cell lines in a hypoxic environment. *Oncol Lett* 6, 1201-1206.

Jiang, S., An, H., Xu, F., and Zhang, X., 2020. Chromosome-level genome assembly and annotation of the loquat (*Eriobotrya japonica*) genome. *Gigascience* 9.

Kim, J. W., Han, K. R., Kim, W., Jung, H. Y., Nam, S. M., Yoo, D. Y., Hwang, I. K., Seong, J. K., and Yoon, Y. S., 2019. Adult Hippocampal Neurogenesis Can Be Enhanced by Cold Challenge Independently From Beigeing Effects. *Front. Neurosci.* 13, 92.

Larson, G., and Fuller, D. Q., 2014. The Evolution of Animal Domestication. *Annu. Rev. Ecol. Evol. S.* 45, 115-136.

Lawal, R. A., Al-Atiyat, R. M., Aljumaah, R. S., Pradeepa, S., Mwacharo, J. M., and Olivier, H., 2018. Whole-Genome Resequencing of Red Junglefowl and Indigenous Village Chicken Reveal New Insights on the Genome Dynamics of the Species. *Front. Genet.* 9, 264-280.

Li, M., Sun, C., Xu, N., Bian, P., Tian, X., Wang, X., Wang, Y., Jia, X., Heller, R., Wang, M., Wang, F., Dai, X., Luo, R., Guo, Y., Wang, X., Yang, P., Hu, D., Liu, Z., Fu, W., Zhang, S., Li, X., Wen, C., Lan, F., Siddiki, A. Z., Suwannapoom, C., Zhao, X., Nie, Q., Hu, X., Jiang, Y., and Yang, N., 2022. De Novo Assembly of 20 Chicken Genomes Reveals the Undetectable Phenomenon for Thousands of Core Genes on Microchromosomes and Subtelomeric Regions. *Mol. Biol. Evol.* 39, msac066.

Lieberman-Aiden, E., Berkum, N. V., Williams, L., Imakaev, M., Ragozcy, T., Telling, A., Amit, I., Lajoie, B. R., Sabo, P. J., and Dorschner, M. O., 2009. Comprehensive Mapping of Long-Range Interactions Reveals Folding Principles of the Human Genome. *Science* 326, 289-293.

Lindsey, B. W., and Tropepe, V., 2014. Changes in the social environment induce neurogenic plasticity predominantly in niches residing in sensory structures of the zebrafish brain independently of cortisol levels. *Dev. Neurobiol.* 74, 1053-1077.

Liu, Y., Su, H., Li, R., Li, X., Xu, Y., Dai, X., Zhou, Y., and Wang, H., 2017. Comparative transcriptome analysis of *Glyphodes pyloalis* Walker (Lepidoptera: Pyralidae) reveals novel insights into heat stress tolerance in insects. *Bmc Genomics* 18, 974-986.

Luger, D., Shinder, D., Wolfenson, D., and Yahav, S., 2003. Erythropoiesis regulation during the development of ascites syndrome in broiler chickens: a possible role of corticosterone. *J. Anim. Sci.* 81, 784-790.

Miao, Y. W., Peng, M. S., Wu, G. S., Ouyang, Y. N., Yang, Z. Y., Yu, N., Liang, J. P., Pianchou, G., Beja-Pereira, A., Mitra, B., Palanichamy, M. G., Baig, M., Chaudhuri, T. K., Shen, Y. Y., Kong, Q. P., Murphy, R. W., Yao, Y. G., and Zhang, Y. P., 2013. Chicken domestication: an updated perspective based on mitochondrial genomes. *Heredity (Edinb)* 110, 277-282.

Pasha, M. Q., Pandey, P., Mohammad, G., and Singh, Y., 2015. ROCK2 and MYLK variants under hypobaric hypoxic environment of high altitude associate with high altitude pulmonary edema and adaptation. *Application of Clinical Genetics* 8, 257-267.

Rafique, S., Thomas, J. S., Sproul, D., and Bickmore, W. A., 2015. Estrogen-induced chromatin decondensation and nuclear re-organization linked to regional epigenetic regulation in breast cancer. *Genome Biol.* 16, 145-163.

- Rao, S. S., Huntley, M. H., Durand, N. C., Stamenova, E. K., Bochkov, I. D., Robinson, J. T., Sanborn, A. L., Machol, I., Omer, A. D., and Lander, E. S., 2014. A 3D map of the human genome at kilobase resolution reveals principles of chromatin looping. *Cell* 159, 1665-1680.
- Shi, S., Shao, D., Yang, L., Liang, Q., Han, W., Xue, Q., Qu, L., Leng, L., Li, Y., Zhao, X., Dong, P., Walugembe, M., Kayang, B. B., Muhairwa, A. P., Zhou, H., and Tong, H., 2022. Whole genome analyses reveal novel genes associated with chicken adaptation to tropical and frigid environments. *J. Adv. Res.*
- Steven, W., Philip, E., Mayra, F. M., Takashi, N., Stefan, S., Peter, F., and Simon, A., 2015. HiCUP: pipeline for mapping and processing Hi-C data. *F1000res* 4, 1310.
- Taberlay, P. C., Achinger-Kawecka, J., Lun, A., Buske, F. A., Sabir, K., Gould, C. M., Zotenko, E., Bert, S. A., Giles, K. A., and Bauer, D. C., 2016. Three-dimensional disorganization of the cancer genome occurs coincident with long-range genetic and epigenetic alterations. *Genome Res.* 26.719-731.
- Takashima, S., 2009. Phosphorylation of myosin regulatory light chain by myosin light chain kinase, and muscle contraction. *Circ. J.* 73, 208-213.
- Tian, S., Zhou, X., Zhang, D., Ning, C., Li, D., and Zhao, H., 2020. Genomic Analyses Reveal Genetic Adaptations to Tropical Climates in Chickens. *iScience* 23, 101644-101658.
- Tjong, H., Li, W., Kalhor, R., Dai, C., Hao, S., Gong, K., Zhou, Y., Li, H., Zhou, X. J., Le Gros, M. A., Larabell, C. A., Chen, L., and Alber, F., 2016. Population-based 3D genome structure analysis reveals driving forces in spatial genome organization. *Proc. Natl. Acad. Sci. U. S. A.* 113, E1663-E1672.
- Veniamin, Fishman, Nariman, Battulin, Miroslav, Nuriddinov, Antonina, Maslova, Anna, and Zlotina., 2018. 3D organization of chicken genome demonstrates evolutionary conservation of topologically associated domains and highlights unique architecture of erythrocytes' chromatin. *Nucleic Acids Res.* 47, 648-665.
- Walsh, M. P., 1994. Calmodulin and the regulation of smooth muscle contraction. *Mol. Cell. Biochem.* 135, 21-41.
- Wang, M., Wang, P., Lin, M., Ye, Z., Li, G., Tu, L., Shen, C., Li, J., Yang, Q., and Zhang, X., 2018. Evolutionary dynamics of 3D genome architecture following polyploidization in cotton. *Nature Plants.* 4, 90-97.
- Wang, M. S., Li, Y., Peng, M. S., Zhong, L., Wang, Z. J., Li, Q. Y., Tu, X. L., Dong, Y., Zhu, C. L., Wang, L., Yang, M. M., Wu, S. F., Miao, Y. W., Liu, J. P., Irwin, D. M., Wang, W., Wu, D. D., and Zhang, Y. P., 2015. Genomic Analyses Reveal Potential Independent Adaptation to High Altitude in Tibetan Chickens. *Mol. Biol. Evol.* 32, 1880-1889.
- Wang, M. S., Thakur, M., Peng, M. S., Jiang, Y., and Zhang, Y. P., 2020. Author Correction: 863 genomes reveal the origin and domestication of chicken. *Cell Res.* 30, 693-701.
- Wang, Y., Guo, F., Pan, C., Lou, Y., Zhang, P., Guo, S., Yin, J., and Deng, Z., 2012. Effects of low temperatures on proliferation-related signaling pathways in the hippocampus after traumatic brain injury. *Exp. Biol. Med.* 237, 1424-1432.
- Wu, P., Li, T., Li, R., Jia, L., Zhu, P., Liu, Y., Chen, Q., Tang, D., Yu, Y., and Li, C., 2017. 3D genome of multiple myeloma reveals spatial genome disorganization associated with copy number variations. *Nat. Commun.* 8, 1937.
- Ying, S. U., Long, Y., Liao, X., Huashui, A. I., Zhang, Z., Yang, B., Xiao, S., Tang, J., Xin, W., and Huang, L., 2015. Detection of genomic signatures for pig hairlessness using high-density SNP data. *Front. Agr. Sci. Engi.* 1, 307-313.
- Zhang, W., Jiao, L., Liu, R., Zhang, Y., Ji, Q., Zhang, H., Gao, X., Ma, Y., and Shi, H. N., 2018a. The effect of exposure to high altitude and low oxygen on intestinal microbial communities in mice. *PLoS One* 13, e0203701.

Zhang, Z., Du, H., Bai, L., Yang, C., Li, Q., Li, X., Qiu, M., Yu, C., Jiang, Z., Jiang, X., Liu, L., Hu, C., Xia, B., Xiong, X., Song, X., and Jiang, X., 2018b. Whole genome bisulfite sequencing reveals unique adaptations to high-altitude environments in Tibetan chickens. *PLoS One* 13, e0193597.

Table 1

Enriched KEGG pathways of DEGs of different A/B compartments between LDC and WCC liver cells

Term	Count	Enriched genes ^a	P-value
Focal adhesion	9	EXOC3, PRKCQ, AMOTL1, CTTN, TJAP1, CLDN16, CLDN1, PRKCH, GNAI2	0.00066
Notch signaling pathway	4	MAML2, ADAM17, JAG2, DTX3L	0.00192
Vascular smooth muscle contraction	8	ADCY5, MYLK, KCNMB1, PRKCQ, PRKCH, ROCK2, MYLK4, GUCY1A2	0.02457
RIG-I-like receptor signaling pathway	4	IFNK, IL8, MAP3K1, FADD	0.03433

^a EXOC3, exocyst complex component 3; PRKCQ, Protein kinase C theta; AMOTL1, Angiomotin-like protein 1; CTTN, Cortactin; TJAP1, Tight junction-associated protein 1; CLDN16, Claudin-16; CLDN1, Claudin-1; PRKCH, Protein kinase C η ; GNAI2, G-protein alpha inhibiting activity polypeptide 2; MAML2, mammalian mastermind like 2; ADAM17, a disintegrin and metalloprotesase 17; JAG2, jagged-2; DTX3L, deltex-3-like; ADCY5, Adenylate Cyclase 5; MYLK, myosin light chain kinase; KCNMB1, Calcium-activated potassium channel subunit beta-1; ROCK2, rho-associated coiled-coil kinase isoform 2; MYLK4, myosin light chain kinase 4; GUCY1A2, Guanylate cyclase soluble subunit alpha-2; IFNK, interferon kappa; IL8, interleukin8; MAP3K1, Mitogen-activated protein kinase kinase kinase 1; FADD, Fas-Associated protein with Death Domain.

Figures

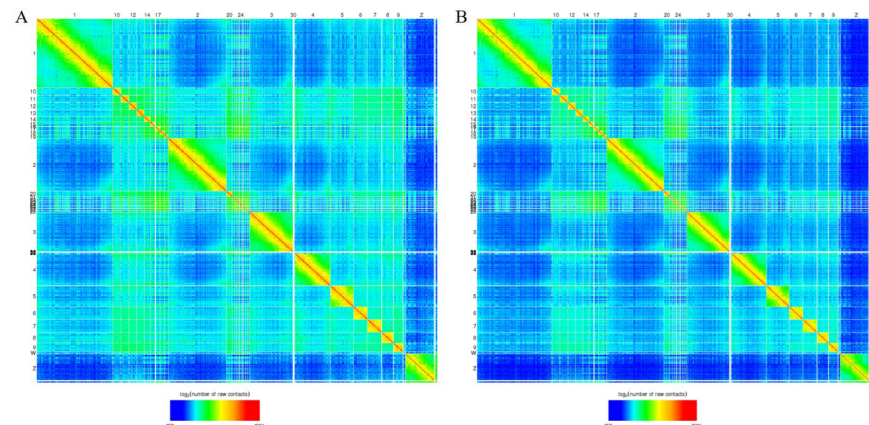


Fig. 1. Hi-C contact heatmaps of liver cells in LDC(A) and WCC(B). The color of each dot on heatmaps represents the log of the interaction probability for the corresponding pair of genomic loci according to

standard JuiceBox color scheme.

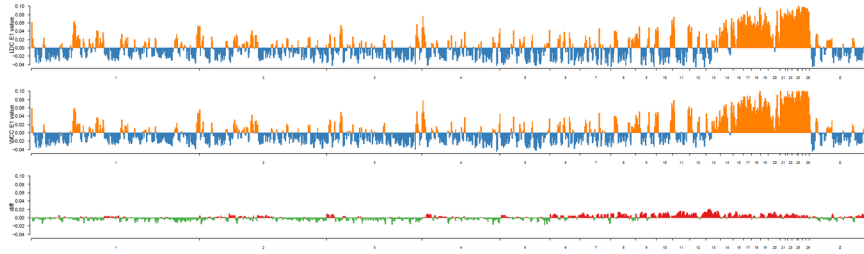


Fig. 2. Distribution of the A/B compartments in the whole genome of two liver cells.

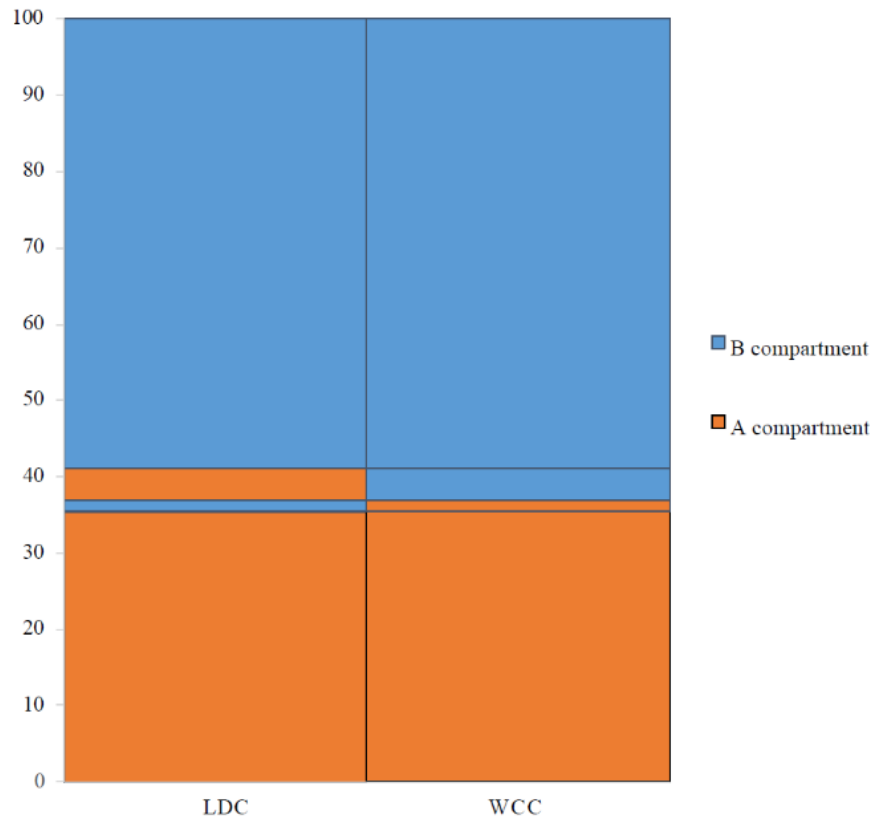


Fig. 3. Genome-wide proportions of A/B compartment changes in the whole genome of two liver cells.

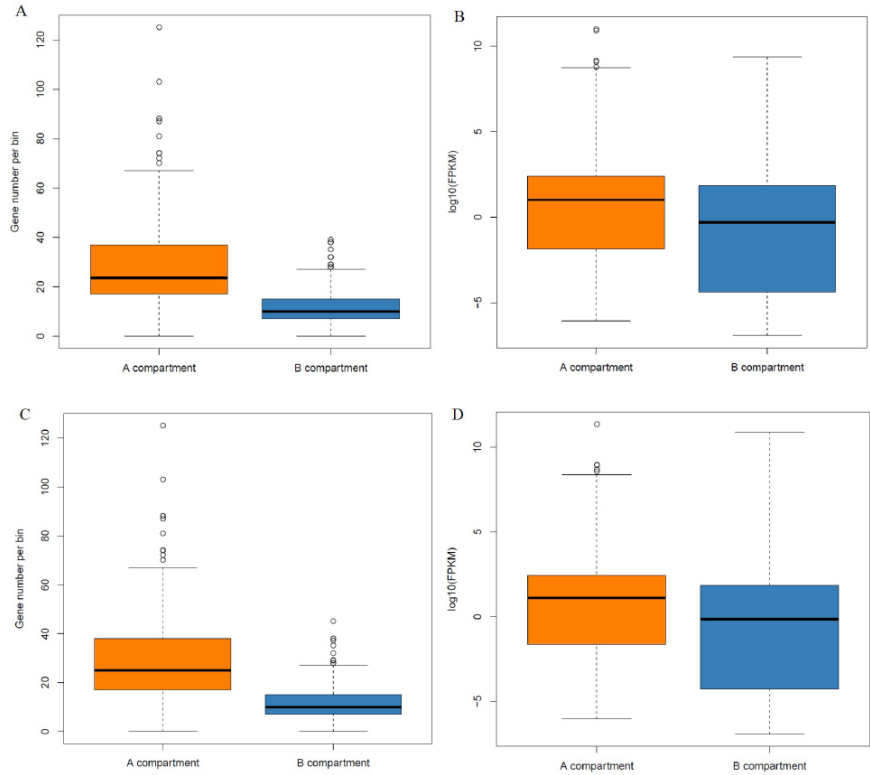


Fig. 4. Gene numbers (A, C) and expression (B, D) volume map of Compartments A/B in the whole genome of LDC and WCC liver cells.

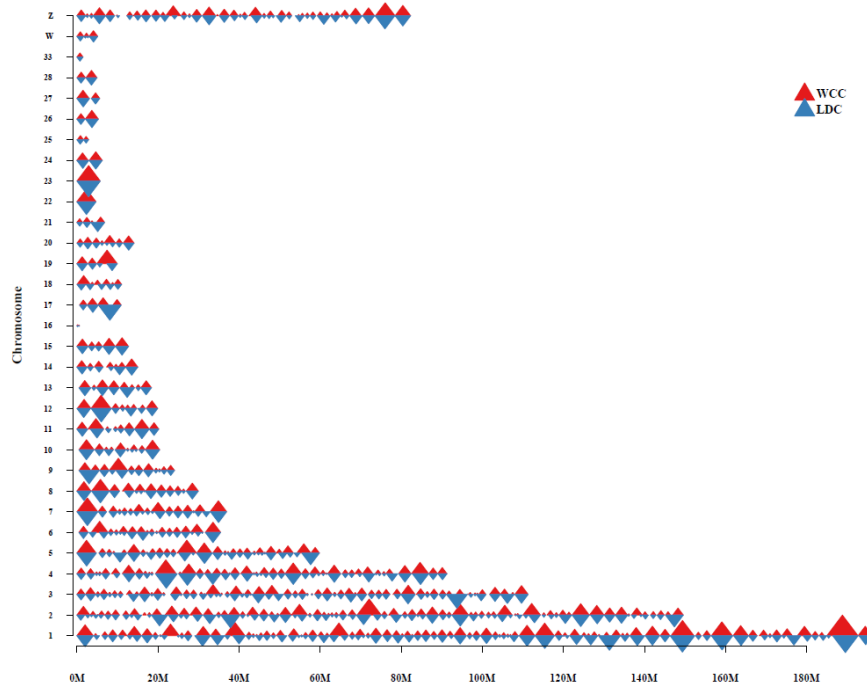


Fig. 5. The distribution of TAD on chromosome.

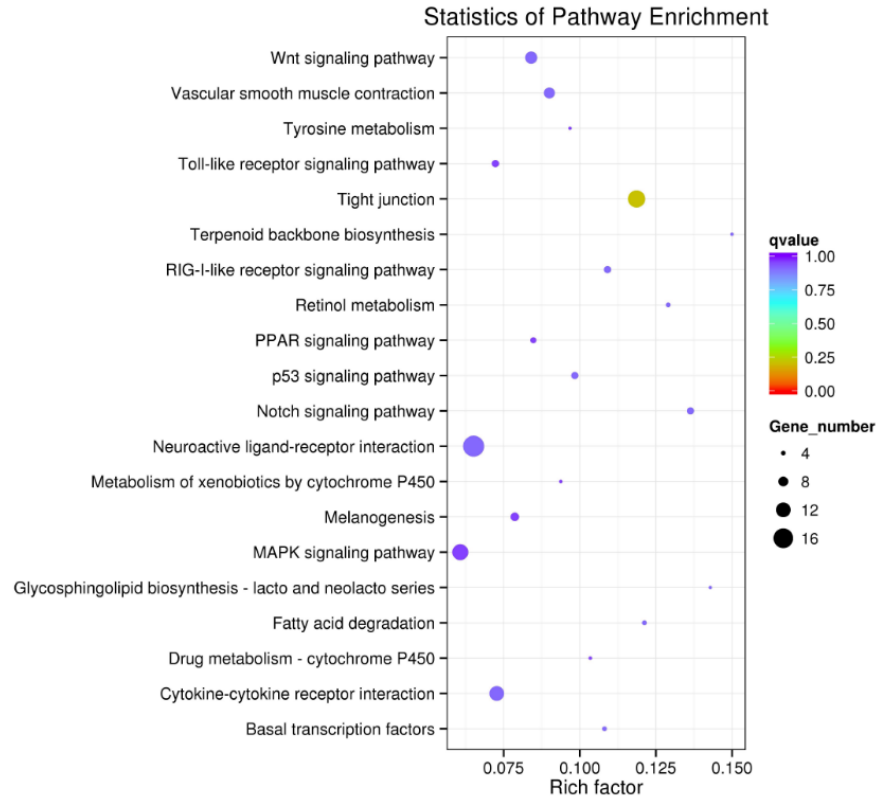


Fig. 6. KEGG enrichment analysis of different A/B compartments between LDC and WCC liver cells. The most 20 KEGG pathways were presented. The y-axis and x-axis indicate pathway name and rich factor, respectively. The size of circle dot means gene number.

Hosted file

4_Supplementary_figure_20220804.docx available at <https://authorea.com/users/508348/articles/586245-3d-organization-of-chicken-genome-demonstrates-evolutionary-conservation-to-extreme-environments>

Hosted file

5_Supplementary_table_20220804.doc available at <https://authorea.com/users/508348/articles/586245-3d-organization-of-chicken-genome-demonstrates-evolutionary-conservation-to-extreme-environments>